



저작자표시-비영리-변경금지 2.0 대한민국

이용자는 아래의 조건을 따르는 경우에 한하여 자유롭게

- 이 저작물을 복제, 배포, 전송, 전시, 공연 및 방송할 수 있습니다.

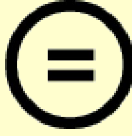
다음과 같은 조건을 따라야 합니다:



저작자표시. 귀하는 원저작자를 표시하여야 합니다.



비영리. 귀하는 이 저작물을 영리 목적으로 이용할 수 없습니다.



변경금지. 귀하는 이 저작물을 개작, 변형 또는 가공할 수 없습니다.

- 귀하는, 이 저작물의 재이용이나 배포의 경우, 이 저작물에 적용된 이용허락조건을 명확하게 나타내어야 합니다.
- 저작권자로부터 별도의 허가를 받으면 이러한 조건들은 적용되지 않습니다.

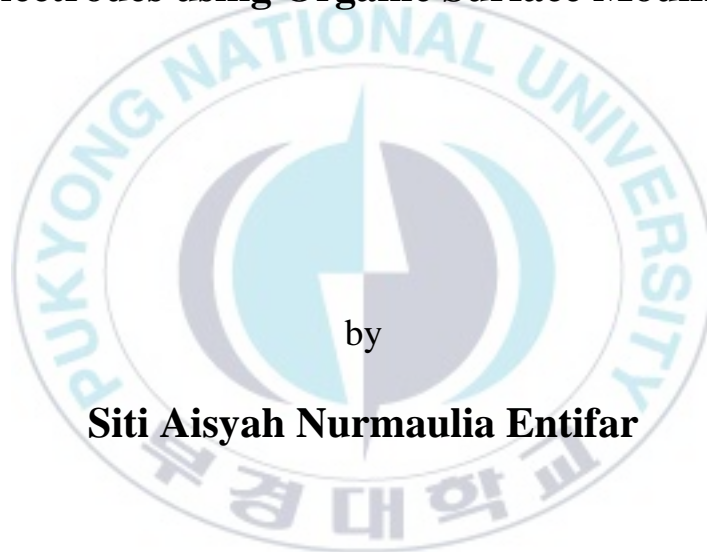
저작권법에 따른 이용자의 권리는 위의 내용에 의하여 영향을 받지 않습니다.

이것은 [이용허락규약\(Legal Code\)](#)을 이해하기 쉽게 요약한 것입니다.

[Disclaimer](#)

**Thesis for the Degree of Master of Engineering**

**Simultaneously Enhanced Optical, Electrical,  
and Mechanical Properties of Highly  
Stretchable Transparent Silver Nanowires  
Electrodes using Organic Surface Modifier**



by

**Siti Aisyah Nurmaulia Entifar**

**Department of Display Engineering,**

**The Graduate School**

**Pukyong National University**

**August, 2018**

**Simultaneously Enhanced Optical, Electrical, and  
Mechanical Properties of Highly Stretchable  
Transparent Silver Nanowires Electrodes using  
Organic Surface Modifier**

유기 표면 개질제를 이용한 신축성 투명한 은 나노와이어  
전극의 광학·전기·기계적 특성 향상 연구

**Advisor: Prof. Yong Hyun Kim**

**By**

**Siti Aisyah Nurmaulia Entifar**

A thesis submitted in partial fulfillment of the requirements for  
the degree of

**Master of Engineering**

**Department of Display Engineering, The Graduate School,  
Pukyong National University**

**August, 2018**

**Simultaneously Enhanced Optical, Electrical, and  
Mechanical Properties of Highly Stretchable  
Transparent Silver Nanowires Electrodes using  
Organic Surface Modifier**

A thesis

by

**Siti Aisyah Nurmaulia Entifar**

Approved by:

---

Yeon Tae Jeong, Ph.D. (Chairman)

---

Kwon Taek Lim (Member)

---

Yong Hyun Kim (Member)

**August, 2018**

## Acknowledge

Firstly, thanks to the merciful Lord, Allah SWT for all the kindness, miracles, and countless gifts which can strengthen me until I finished this study.

I would like to show my gratitude to my advisor, Professor Yong Hyun Kim, whose expertise, understanding, patiently, generous guidance, his support, and encouragement regardless of my absurd ideas and how slow my thinking was. His unrelenting encouragement to let me do anything and everything in our laboratory freely where I did repeat mistakes and failures which is certainly very fundamental useful in my ability before finally discovering and got a result. One more time, thank you for my Professor who provided me with the knowledge, skills, and insight needed to be a successful engineer made it possible for me to study and did the research on a fascinating topic that I never knew before will be useful for my future.

I would also like to thank the following professors, Professor Lim Kwon Taek, Professor Jeong Yeon Tae, Professor Chang Dong Wook, Professor U Hyeok Choi for their guidance and gave me a chance to join their class so I got more knowledge and officers in the department of Display Engineering Mrs. Su Kyeong and Ms. Bo Ram who always help me to comply with all of the necessary during my study.

Besides the above, there is another one I want to say so many thank you. They are my lovely lab mates in Organic Semi-Conductor Material and Devices Laboratory:

- Han Joo Won, our motherly person and able to solve all kinds of problems that appear here, she's my first Korean friend and who has always been with me for 2 years.

- Lee Dong Jin, a very pleasant guy and gives a positive aura to others, he always jokes so that others are happy, includes me and he always helps others without ulterior motives.

- Zeno Rizqi Ramadhan, he also very kind, and the most important thing, he never angry at others even though sometimes the situation was not good.

- Hong Ju Hee, the cutest girl in this lab, with her confident she always said: "she is beautiful". And she always disturbs me, so I will remember you. But, behind it all, she is very kind and gives the happiness to others especially for me.

- Seo Jin Ju, the youngest in our lab, she is beautiful and also cheerful. Keep your joy to make others happy.

Became first foreigner is not an easy thing, so without them, I was nothing. Their help, care, and encouragement have been especially valuable to pursue the success of my study in here. They gave me a comfortable and good work environment for the last two years. Also, other friends in this department who always care and make me feel like having a family like Eun Mi, Cuong, Trang, Thang, Ming Kyo, Dong Woo, Han Eun, Won Tae.

On a more personal note, I would like to thank the friends in Pukyong National University especially Mutia, Sabrina, Prita, Sella, Ratna, Nico, Andi, Aldias, Affandy, Majid, Fauzy, Daru and so many others with whom I'm lucky enough to spend my time outside of the lab for all of their support during the ups and downs of graduate school. The great people I've met while at Pukyong have been there both for the fun and for the complaints, and I am lucky to have met and to have spent time with such great people. They always help me in every day I need them, always listen to my ridiculous story and have supported me throughout the entire process. They never wrong to give happiness to me. I will be grateful forever for our friendship.

I will not forget to say many thanks to my best friend, Alif, Tya and Dhuha also my besties, Dina, Fitria, Anita, Icha, Desvia, Annas who always listen to my story and give support for me.

I would like to thank you to Arifin Budiman, someone who has the special way to support me.

The last but not least, my great gratitude I dedicate to my family, my father Faridj Asjari, my mom Endang Sriwiyati and my sister Ellena, are really the most important people in the world to me, and without them I would certainly have never finished this work, nor would I be where I am today. They always supported my every endeavor since the day I was born, and their help, wisdom, advice, love, and values that they have instilled in me have been the driving forces for every success that I had in life. I love and appreciate them very much. I hope that my family can be proud of me, both here, academically, and in the future.

## Table of Contents

Cover.....	
Acknowledge .....	i
Table of Contents .....	iii
List of Figures .....	v
List of Abbreviation.....	v
Abstract.....	x
요약 (Korean Abstract).....	xi
Chapter 1 INTRODUCTION.....	1
Chapter 2 THEORITICAL BASIS .....	5
2.1. Optoelectronic Devices .....	5
2.2. Background of Flexible and Stretchable Electronics. ....	6
2.3. Transparent Electrode .....	8
2.3.1. Indium Tin Oxide (ITO) .....	10
2.3.2. Carbon Nanotubes (CNTs).....	12
2.3.3. Graphene .....	15
2.3.4. Conductive Polymer; PEDOT: PSS.....	29
2.3.5. Silver Nanowires (AgNWs).....	18
2.3.5.1. AgNWs electrode challenge.....	21

Chapter 3 EXPERIMENTAL DETAILS.....	23
3.1. Experimental Section .....	23
3.2. Measurement .....	25
Chapter 4 RESULT AND DISCUSSION.....	26
4.1. Surface Modifier for Transparent Electrode .....	26
4.2. Optical and Electrical Properties of Transparent Electrode .....	27
4.3. Mechanical Stability of the Electrode .....	31
4.4. Chemical and Air Exposure Stability of the Electrode	49
4.5. Performance of Transparent Electrode in Transparent Heater.....	37
4.6. Performance of Transparent Electrode in ACEL Device .....	42
Chapter 5 CONCLUSION .....	44
Chapter 6 REFERENCES .....	57

## List of Figures

<b>Figure 1.</b> Flexible optoelectronic devices .....	6
<b>Figure 2.</b> UV–vis transmittance and the absorption spectrum of ITO thin films. Inserted image shows the blue shift of absorption edges in various doping level <sup>26</sup> . .....	11
<b>Figure 3.</b> SEM image of the crack on the ITO layer with strain of 2% <sup>23</sup> .....	11
<b>Figure 4.</b> Structure of (a) SWCNT, (b) DWCNT, and (c) MWCNT. Note: SWCNT, single-walled carbon nanotube; DWCNT, double-walled carbon nanotube; MWCNT, multiwalled carbon nanotube <sup>42</sup> .....	13
<b>Figure 5.</b> Photograph and SEM image of the CNTs <sup>44</sup> .....	14
<b>Figure 6.</b> Sheet resistance versus transmittance for SWNT films with varying thicknesses, before and after oleum treatment <sup>45</sup> ....	15
<b>Figure 7.</b> (a) Electrical conductivity as a function of transmittance at a wavelength of 550 nm at different stages of treatment <sup>46</sup> (b) SEM image of the initial graphite flakes <sup>50</sup> . .....	16
<b>Figure 8.</b> Chemical Structure of PEDOT: PSS .....	18
<b>Figure 9.</b> SEM micrographs for AgNWs deposited on hydroxylated PDMS: panels a–e are low magnification and panels f–j high magnification images. Panels a and f represent the pristine state, b and g the 25% strain stretched state, c and h the	

50% strain stretched state, d and i the 75% strain stretched state, and e and j show images during stretching at 100% strain<sup>61</sup>. ..... 20

**Figure 10.** Sheet resistance and transmittance of silvernanowires based on references<sup>62-75</sup>. ..... 20

**Figure 11.** Schematic illustration of the fabrication process of electrode and Pre-treatment mechanism using Plasma Treatment and 11-Aminoundecanoic Acid ..... 24

**Figure 12.** Schematic structure of ACEL devices..... 25

**Figure 13.** Schematic illustration of the formation of chemical bonds with 11-AA between the AgNW and the PDMS substrate. .... 27

**Figure 14.** Sheet resistance and transmittance of AgNWs in various spin speed ..... 29

**Figure 15.** Sheet resistance and transmittance of (a) AgNW and (b) c-AgNW treated with various concentration of 11-AA. .... 30

**Figure 16.** (a) Changes of resistances for c-AgNW treated with various concentration of 11-AA under tensile strains. (b) Photographs of c-AgNW under stretching and bending conditions. .... 33

**Figure 17.** SEM images of stretched c-AgNW treated with 0.14 wt.% of AA under various tensile strains. .... 34

**Figure 18.** Changes of the normalized resistance for AgNW and c-AgNWs which is dipped in ethanol ..... 36

**Figure 20.** Changes of the normalized resistance for AgNW and c-AgNWs which is exposed in air ambient..... 37

<b>Figure 21.</b> Temperature changes of STHs based on AgNW and c-AgNW as a function of time with increased applied voltages. Inset shows dynamic temperature control of the STHs with AgNW and c-AgNWs .....	39
<b>Figure 22.</b> The stability of heater with heating and cooling test with time interval 100 s in 10 min. ....	39
<b>Figure 23.</b> (a) IR image of the STH with c-AgNW under various tensile strains. (b) Photograph and IR image of STH with c-AgNW attached on a vial. (c) (d) (e) Photographs and IR images of STHs based on c-AgNW under twisting and bending conditions. ....	41
<b>Figure 24.</b> Photographs of ACEL device with a frequency 400 Hz (left) and 1000 Hz (right) and a voltage of 400 V.....	42
<b>Figure 25.</b> (a) Electroluminescent intensity (at 500 V) and (b) luminance (at 400 Hz) of the stretchable alternating current electroluminescence device.....	43

## List of Abbreviation

TCE	Transparent conductive electrode
TCOs	Transparent conductive oxides
ITO	Indium tin oxide
AgNWs	Silver Nanowires
CNTs	Carbon Nanotubes
SWCNTs	Single-wall carbon nanotubes
DWCNTs	Double-wall carbon nanotubes
MWCNTs	Multi-wall carbon nanotubes
ZnO	Zinc Oxide
PEDOT: PSS	poly(3,4-ethylenedioxythiophene): poly(styrenesulfonate)
PDMS	Polydimethylsiloxane
PET	Poly ethylene terephthalate
11-AA	11-Aminoundecanoic Acid
OLED	Organic light emitting diodes
LCD	Liquid Crystal Display
EL	Electroluminescent
ACEL	Alternating current electroluminescent
STH	Stretchable transparent heater
DIW	Deionized Water

sq	Square
nm	Nanometer
s	Second
min	Minute
SEM	Scanning electron microscope



**Simultaneously Enhanced Optical, Electrical, and Mechanical  
Properties of Highly Stretchable Transparent Silver  
Nanowires Electrodes using Organic Surface Modifier**

**Siti Aisyah Nurmaulia Entifar**

Departement of Display Engineering, The Graduate School  
Pukyong National University

**Abstract**

We report on a new surface modifier which simultaneously improves electrical, optical, and mechanical properties of silver nanowire-based stretchable transparent electrodes. The transparent electrodes treated with 11-aminoundecanoic acid achieve a low sheet resistance of 26.0  $\Omega$ /sq and a high transmittance of 89.6 % with an excellent stretchability. These improvements are attributed to the effective formation of a strong chemical bond between silver nanowire networks and elastomeric substrates by 11-aminoundecanoic acid treatment. The resistance changes of the optimized silver nanowire/PEDOT: PSS thin-films is only about 10 % when stretched by 120 %. In addition, the chemical stability of stretchable silver nanowire films are significantly improved by the introduction of conductive poly(3,4-ethylenedioxythiophene): poly(styrenesulfonate) (PEDOT: PSS) overcoat film. The optimized electrodes are utilized as high performance stretchable transparent heaters, successfully illustrating its feasibility for future wearable electronics.

# 유기 표면 개질제를 이용한 신축성 투명한 나노와이어

## 전극의 광학·전기·기계적 특성 향상 연구

Siti Aisyah Nurmaulia Entifar

부경대학교 대학원융합디스플레이공학과

### 요약

우리는 나노 와이어 기반의 신축성 있는 투명 전극의 전기, 광학 및 기계적 특성을 동시에 향상시키는 새로운 표면 개선제에 대해 보고한다. 11-aminoundecanoic acid 로 처리 된 투명 전극은  $26.0 \Omega / \text{sq}$  의 낮은 시트 저항과 89.6 %의 높은 투과율을 달성한다. 이러한 향상은 11-aminoundecanoic acid 처리에 의한 은 나노 와이어 네트워크와 엘라스토머 기질 사이의 강한 화학적 결합의 효과적인 형성에 기인한다. 또한 (poly (3,4-ethylenedioxythiophene): poly(styrenesulfonate) (PEDOT: PSS)의 수많은 코팅 도입으로 신축성 있는 은 나노 와이어 필름의 화학적 안정성과 신축성이 크게 향상되었다. 최적화된 은 나노 와이어 / PEDOT : PSS 박막은 120% 늘어뜨렸을 때 약 10%의 저항 변화가 있었다. 최적화된 전극은 고성능 신축성 투명 히터로 활용되어, 미래 웨어러블 장치에 대한 가능성을 성공적으로 보여준다.

## Chapter 1

### INTRODUCTION

High performance stretchable transparent conductive electrodes (TCEs) are of great necessity for the development of stretchable optoelectronics, which can be integrated in devices with new form factors, such as textiles, skin-based devices, and wearable devices<sup>1,2</sup>. Indium tin oxide (ITO) is the most generally used TCE in optoelectronics such as organic light-emitting diodes and various solar cells owing to its high optical transmittance and high electrical conductivity. However, the application of ITO is strongly limited in stretchable electronics due to its high costs, inherent brittleness, and high-temperature manufacturing process<sup>3</sup>. Graphenes<sup>4,5</sup>, carbon nanotubes<sup>6,7</sup>, conductive polymers<sup>8,9</sup>, metal grid<sup>10,11</sup>, and metal nanowires<sup>12,13</sup> have thus been widely investigated as alternative TCEs to replace ITO. As an ideal stretchable electrode for wearable electronic devices, however, these alternative TCEs still suffer from a number of challenges including high electrical resistance or poor stretchability on stretchable substrates. Silver nanowires (AgNWs) is one of the promising stretchable TCE because it offers high conductivity, high

transmittance, and good mechanical performances, and easy solution processability<sup>14</sup>. The AgNWs networks achieve a sheet resistance and a transmittance comparable to those of ITO. With these excellent electrical and optical properties of AgNWs, there have been many studies for applications of AgNWs-based TCE in organic solar cells, organic light-emitting diodes, touch panels, transistors, and stretchable electronic devices<sup>14-16</sup>.

The approaches in achieving stretchable electrodes can be described as follows; (i) deposit conductive materials with new structural layouts such as wavy, meshed, percolated, or buckled geometries on an elastomeric substrate or (ii) deposit conductive materials in surface-modified elastomeric substrates<sup>15,17</sup>. The AgNWs networks as well as other TCEs are generally unsuitable for stretchable applications due to inherent brittleness, rigidness, and poor adhesiveness on highly hydrophobic surfaces of elastomeric substrates such as polydimethylsiloxane (PDMS), most widely used stretchable substrates. Moreover, the TCE films can be easily peeled-off from the elastomeric substrate when small mechanical forces are applied. However, there have been a few studies especially for AgNWs to overcome such issue, up to now. Exposure to oxygen plasma or introduction of

aqueous hydrochloric acid are ways to realize defined surface properties of elastomeric substrate<sup>13,17-19</sup>.

In this study, we report simultaneously improved electrical, optical, and mechanical properties of AgNWs-based stretchable TCE by incorporating 11-aminoundecanoic acid (11-AA) as the novel surface modifier processed by simple spin-coating. The TCEs treated with 11-AA achieve a low sheet resistance of 26.0  $\Omega$ /sq and a high transmittance of 89.6 %. This high performance is attributed to the effective hydrogen and covalent bonding formed between AgNWs networks and highly hydrophobic PDMS substrates with 11-AA. Furthermore, we develop 11-AA-treated AgNWs/conductive poly(3,4-ethylenedioxythiophene): poly(styrenesulfonate) (PEDOT: PSS) composites, resulting in the enhanced chemical stability and stretchability of stretchable thin-films. The change of resistance for AgNWs/PEDOT: PSS hybrid electrodes optimized with 11-AA is only 11% under a strain of 120 %. With the use of 11-AA, the electrical property is retained at high tensile strains and repeated stretching conditions. In addition, the optimized composite TCEs are utilized to transparent heaters, showing much enhanced Joule heating performance. The stretchable devices exhibit superior elastic behaviors, which can be

stretched, bent, and twisted without performance degradation. The AgNWs optimized with 11-AA treatment and overcoating PEDOT: PSS can provide a new path toward high performance stretchable transparent electrodes for robust stretchable electronics.



## Chapter 2

### THEORITICAL BASIS

#### 2.1. Optoelectronic Devices

In the 21<sup>st</sup> century, many technologies were improved day by day, especially in the field of optoelectronic devices. Optoelectronics is an interesting branch of electronics that combines both electronics and optics. Optoelectronic devices find varied applications in telecommunications, military services, medical field, and automatic control systems such as organic solar cells, organic light-emitting diodes, touch panels, transistors, and stretchable electronic devices. In the last decade, the market for electronic displays and touchscreens has increased drastically. For example, 362 million touch panels were produced in 2010 with an increase of 20% each year up to 2014<sup>20</sup>. Besides the touch panel, the consumption of solar cells also increased. In 2005, Nobel laureate Dr. Richard Smalley discussed about “Terawatt Challenge” and he suggested that solar power is the best sustainable energy which is can produce 125.000 terawatts/year<sup>21</sup>. Besides touch panels and solar cells, OLEDs also have a high attention nowadays, Jean-Francois Tremblay predicted that the OLED display market will grow

quickly, it will be increased from \$16 billion in 2016 to \$42 billion in 2020. OLED displays can be lighter, they can be flexible, and they allow designers more leeway with the shape of their devices,” says Guillaume Chansin, senior technology analyst at IDTechEx.



**Figure 1.** Flexible optoelectronic devices

## **2.2. Background of Flexible and Stretchable Electronics.**

Nowadays, the flexible and stretchable electronic has been popular due their opportunity to produce the great devices, especially in optoelectronics field. In here, the definition of strength which is needed for a material where if it will be applied stress there is no failure of the devices. Stress of a device can be caused by the external factors and internal physical process. The normal stress like compression or tension can make a failure of the active

area. There is some relation between strength and the material ability like compressive strength can show the ability of material for resist pressure, tensile strength relates to the ability to resist pulling, and the shear strength relates to the ability to resist sliding<sup>22</sup>. Some example of the failure of the devices like cracking, sliding, delamination, debonding and channeling should be overcome. Another possibility of damage to flexible devices may be due to significant temperature differences occurring in an optoelectronic device. The high temperature of devices can cause the failure of the interconnection in the electrode layer. In the case of the conductor material, the degree of adhesion of the material which is deposited in the substrate determines the mechanical stability of the composite. If the substrate is hydrophobic and the adhesion between the conductive material and substrate is weak, the film will slide against the substrate at a certain stress to reduce the strain localization. This is because the strain concentrated on a small region can cause a debonding. In contrast, a polymer substrate with strong interfacial adhesion to the conductive film can effectively delocalize the strain.

### 2.3. Transparent Electrode

One of the important parts of the electronic or optoelectronic devices is transparent electrode film which has electrical properties and high optical transparency. Some devices which are needed transparent electrodes such as touch sensors, organic light emitting diodes (OLED), organic solar cells, electroluminescent devices (EL), liquid crystal displays (LCDs), smart windows and transparent heaters. For example, in OLEDs and organic solar cells device, transparent electrode was needed as the cathode and anode for connecting the circuit in device. Based on materials used, transparent electrode is divided into 4 types:

- a. Transparent conductive oxides (TCOs); Doped metal oxides ex. indium tin oxide (ITO), aluminum-doped zinc oxide (AZO), zinc oxide (ZnO), fluorine doped tin oxide (FTO), and indium doped zinc oxide (IZO).
- b. Carbon based system: graphene, carbon nanotubes (CNTs), highly n-doped C<sub>60</sub>.
- c. Metal based system: metal grids, metal nanowires, thin metal films, dielectric-metal-dielectric sandwich.
- d. Conductive polymers: PEDOT: PSS.

The common material as transparent electrode is ITO because it has some great properties like a low sheet resistance and high transparency, but ITO cannot cover all the new expected qualifications for the new generation optoelectronic devices. The most important is the mechanical properties of ITO, ITO has ceramic properties which make ITO is brittle and not flexible, 2-3% of strain can initiate the crack in ITO film on flexible substrate, which reduces the conductivity of electrode and the performance of ITO<sup>23</sup>. Besides that, the high price of raw material for ITO that is indium is volatile with an overall increasing trend<sup>24</sup>. Then, the fabrication process of ITO needed a high cost because it requires the high temperatures and high vacuum for control over the thickness and doping concentration<sup>24</sup>. Last, ITO has a high refractive index of refraction, it is not suitable for display applications because it reflects light which decreasing the brightness of the screen, so the additional material needs to be applied to solve the problem and leading to additional cost.

For transparent electrode, simultaneously of sheet resistance and optical transmittance is the most important parameter that must be defined in optoelectronic devices. The minimum standard required for transparent electrode is  $T \geq 90\%$  and  $R_s < 100 \Omega$ <sup>25</sup>.

### 2.3.1. Indium Tin Oxide (ITO)

ITO was nominated as the most outstanding material for the transparent electrode which is used in the optoelectronic devices. It happened because of ITO have great properties like a high conductivity until  $10^4$  S/cm<sup>-1</sup>, very low sheet resistance  $24 \Omega/\text{sq}$ , and it also shows the high transparency 80% visible range 360nm~800nm<sup>26</sup>. Films of transparent conductive oxides can be transparent to visible light because of the band gap energies are higher than the energy of photons in the visible range. With the band gap  $>3.8$  eV, ITO can absorb a large portion of light with wavelengths below 300nm<sup>26</sup>. ITO was synthesized by doping indium oxide ( $\text{In}_2\text{O}_3$ ) with tin (Sn). In the fabrication process of thin film with ITO material, many methods can be applied like jet nebulizer spray pyrolysis<sup>26</sup>, magnetron sputtering<sup>27,28</sup>, sol-gel process<sup>29,30</sup>, thermal evaporation<sup>31</sup>, pulsed laser deposition<sup>32,33</sup>, ink-jet printing<sup>34</sup>, and chemical spray deposition<sup>35</sup>. The optical properties of the thin film were depending on the thickness, microstructure, level of impurities and deposition parameters. The film which is thicker will has a high conductivity, but low transmittance.

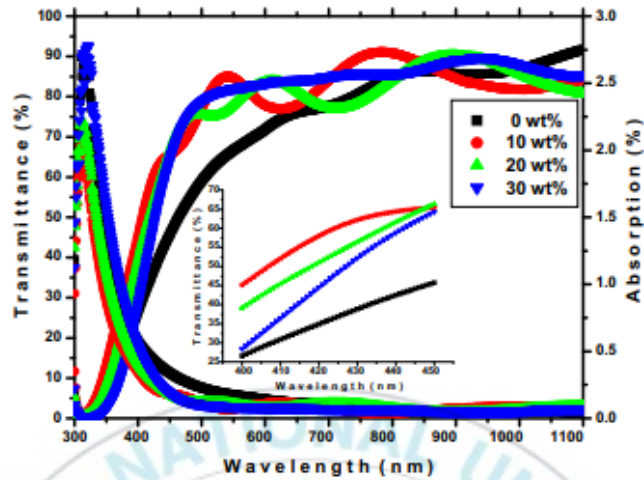


**Figure 2.** UV-vis transmittance and the absorption spectrum of ITO thin films. Inserted image shows the blue shift of absorption edges in various doping level<sup>26</sup>.

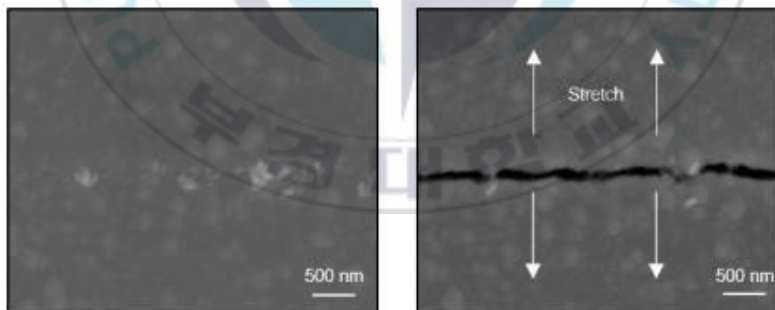


**Figure 3.** SEM image of the crack on the ITO layer with strain of 2%<sup>23</sup>.

With the disadvantages of ITO, like inherently brittle and low number of the strain because ITO has a ceramic property<sup>36</sup>. Besides that,

ITO is not chemical stable<sup>37</sup> and has poor transmittance in the blue visible regime<sup>38</sup>. Furthermore, the raw material of ITO that is indium is very expensive cost of \$565/kg in 2008 and it will increase until \$3000/kg. The last is the typically deposited process of ITO onto substrate by sputtering process and it was an inefficient process which requires high temperature and high vacuum condition for control the thickness and doping concentration<sup>39,40</sup>. Several alternative materials for transparent electrode have been investigated like carbon nanotubes, graphenes and silver nanowires. To produce some excellent devices, the flexibility, simple fabrication process, low cost, and lightweight was needed.

### **2.3.2. Carbon Nanotubes (CNTs)**

First time, CNTs has been investigated in 1900 and CNTs has much attraction in material for conducting material for electrodes. CNTs are cylindrical nanostructure which is consisting of carbon and it has the special physical properties like high surface area, low mass density, high electrical conductivity and remarkable chemical stability<sup>24</sup>. Usually, CNTs was categorized into three types, single-wall carbon nanotubes (SWCNTs), double-wall carbon nanotubes (DWCNTs) and multi-wall carbon nanotubes

(MWNTs). SWCNTs have the diameter ranging from 0.4 to 3 nm with simple geometry. They can be formed by the rolling up of graphene sheets. MWCNT consists of concentric arrays of several cylinders with diameter of about 100 nm. Double-walled carbon nanotube (DWCNT) is the special type of MWCNT consisting of two concentric cylinders<sup>41</sup>.

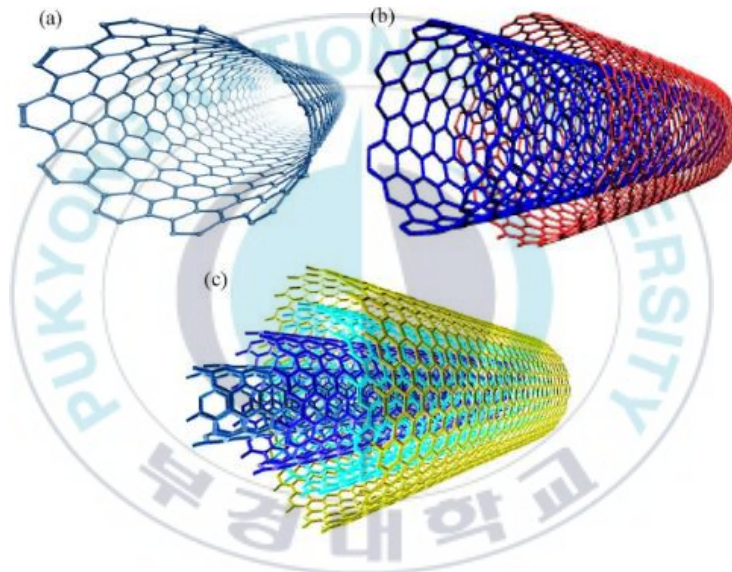


**Figure 4.** Structure of (a) SWCNT, (b) DWCNT, and (c) MWCNT. Note: SWCNT, single-walled carbon nanotube; DWCNT, double-walled carbon nanotube; MWCNT, multiwalled carbon nanotube<sup>42</sup>

The SWCNTs, DWCNTs, and MWCNTs fabricated by various methods, like electrolysis, Arc discharge, Laser ablation, sonochemical or hydrothermal and chemical vapor deposition which is categorized to hot

filament, water assisted, oxygen assisted, microwave plasma, radio frequency, thermal and plasma enhanced<sup>42</sup>. Each method has their own advantages and disadvantages in CNTs properties like inner and outer diameter, and number of walls<sup>43</sup>.

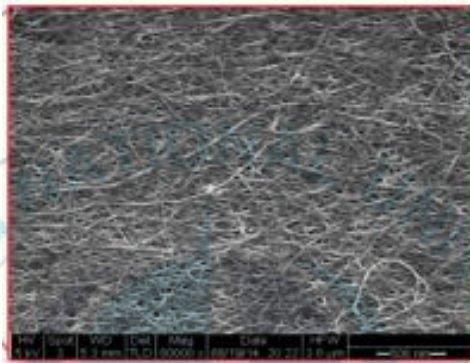


**Figure 5.** Photograph and SEM image of the CNTs<sup>44</sup>

The random networks of CNTs have a purpose as an alternative material to ITO, however, the conductivity of CNTs are lower than ITO because of high resistance at the junction of overlapping nanotubes in the network. Some treatments have been introduced to reduce the sheet resistance of CNTs such as treating using longer CNTs and treating with acid<sup>24</sup>. In figure, showed the reducing of sheet resistance of CNTs after the acid treatment, in number of transparency 80%, the sheet resistance  $\pm 500 \Omega/\text{sq}$  and after acid treated  $R_s$  reduce to  $140 \Omega/\text{sq}$ .

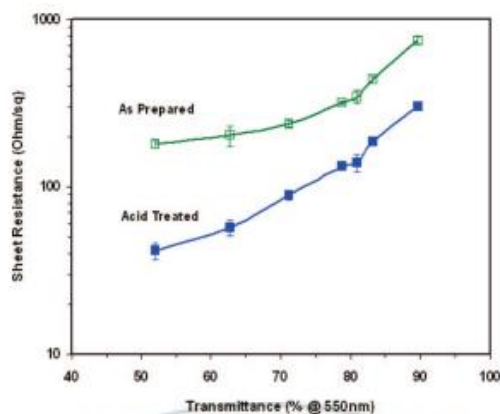


**Figure 6.** Sheet resistance versus transmittance for SWNT films with varying thicknesses, before and after oleum treatment<sup>45</sup>.

### 2.3.3. Graphene

The one of popular material for transparent electrode is graphene. Around the year 2010, research on graphene began widely done by researchers in the world. Basically, graphene is a single atomic layer of graphite where graphene is abundant mineral which is an allotrope of carbon made from very strong bonded carbon atoms organized into a honeycomb lattice. The specialty of graphene is two dimensional which is atomically sheet of sp<sup>2</sup> hybridization with thickness 0.345nm. Then, graphene attracted much attention from researchers in this field, graphene released as the material of transparent electrode, graphene unusual physical and mechanical properties of graphene, like high a thermal conductivity, high mechanical

stability, high carrier concentration and mobility also along with a room temperature quantum hall effect which is comparable with ITO<sup>46</sup>. Graphene materials can be synthesized in several techniques into various morphologies such as kept suspended in solution<sup>47</sup>, configured into paperlike materials<sup>48</sup>, and incorporated into polymer or glass/ceramic nanocomposites<sup>49</sup>. Based on research, graphene film was successfully produced with transparency 80% and electrical conductivity over 200 S/cm (Rs 1-2 K $\Omega$ /sq). The lowest sheet resistance achieved in this study was 181.2  $\Omega$ /sq (or electrical conductivity = 649 S/cm) with a transmittance around 35% at a wavelength of 550 nm<sup>46</sup>. These flakes result in very high sheet resistance, in the range of several k $\Omega$  the high contact resistance between flakes have happened so the overall conductivity is low.

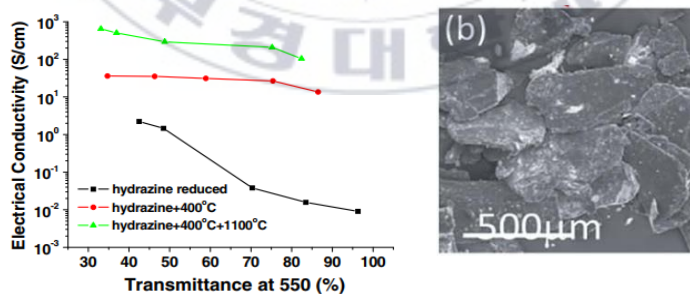


**Figure 7.** (a) Electrical conductivity as a function of transmittance at a wavelength of 550 nm at different stages of treatment<sup>46</sup> (b) SEM image of the initial graphite flakes<sup>50</sup>.

#### 2.3.4. Conductive Polymer; PEDOT: PSS

Conductive polymer named PEDOT: PSS poly(3,4 ethylenedioxythiophene): poly(styrenesulfonate) have a big attention in transparent conductive materials field because it has interesting properties like high transparency and high conductivity, besides that PEDOT:PSS has an excellent mechanical stability and the last one PEDOT: PSS easy aqueous solution processing<sup>51</sup> and compatibility with low-cost solution processing<sup>52</sup>. Electrical conductivity of pristine PEDOT: PSS is below 1 S/cm, but many methods can be applied for increasing it. The common method was used polar organic compounds having a high boiling point like ethylene glycol (EG) and dimethyl sulfoxide (DMSO), it can be increased the conductivity higher than 700 S/cm<sup>8</sup>. Besides that, mannitol, ionic liquids, acids, anionic surfactant, ultrasonic method, and in-situ grafting method in PEDOT: PSS solution also increases the conductivity<sup>53-56</sup>. Post-treatment of PEDOT: PSS with solvent like methanol, hexafluoroacetone or sulfuric acid will be improved the conductivity<sup>57,58</sup>. Highly conductive PEDOT: PSS transparent electrodes was achieved with prepared 2-ethoxyethanol as solvent for post-treatment. The electrical conductivity increased to 1417 S/cm and greatly reducing of sheet resistance from 312.5 to 210.7  $\Omega$ /sq after solvent post-

treatment happened<sup>52</sup>. With this properties, OLED which has a similar qualification with ITO successfully made<sup>52</sup>. Besides OLED, transparent heater also successfully made with PEDOT: PSS as transparent electrode with post-treatment by ethylene glycol in transparency 89.6% and sheet resistance 68  $\Omega$ /sq show the excellent heating performance. In 12 volt of current, 110 °C of heat can be reached in 200 s and the stability of transparent heater with applied voltage 5 volt more than 250 min<sup>59</sup>.

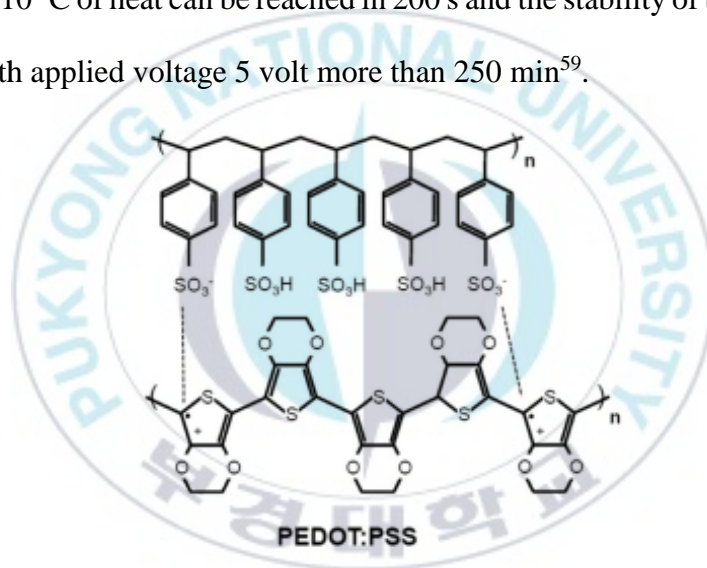


**Figure 8.** Chemical Structure of PEDOT: PSS

### 2.3.5. Silver Nanowires (AgNWs)

AgNWs became the most promises material for the transparent electrode now time. As the transparent electrode, AgNWs present the low resistance, high transparency and the outstanding mechanical stability of

AgNWs has been investigated in many references. AgNWs can be synthesized in solution with the polyol method. In this method, ethylene glycol (EG) solution of poly (vinyl pyrrolidone) (PVP), NaCl and AgNO<sub>3</sub> is used as the materials. EG and NaCl heated in 170 °C and then mixed with AgNO<sub>3</sub> for creation of Ag<sup>+</sup>, and in the result, it will produce the nanoparticles due to homogeneous nucleation. PVP has a strong interaction with facets and passivates these surfaces, and it makes the slows down the addition of Ag. Then, facets grow faster and produce 1D wire structure. This method results in pentagonal shape silver nanowires, including a 5-fold grain structure<sup>60</sup>. AgNWs trusted has a high flexibility, for example in PDMS substrate, AgNWs can be strain up to 150% and it can be strain stretch and release testing in 50% until 1000 times with increasing of sheet resistance less than 50%<sup>61</sup>. It supported by SEM results showed in Figure 9. Based on references, the electrical and optical characteristic of AgNWs showed in the Figure 10.

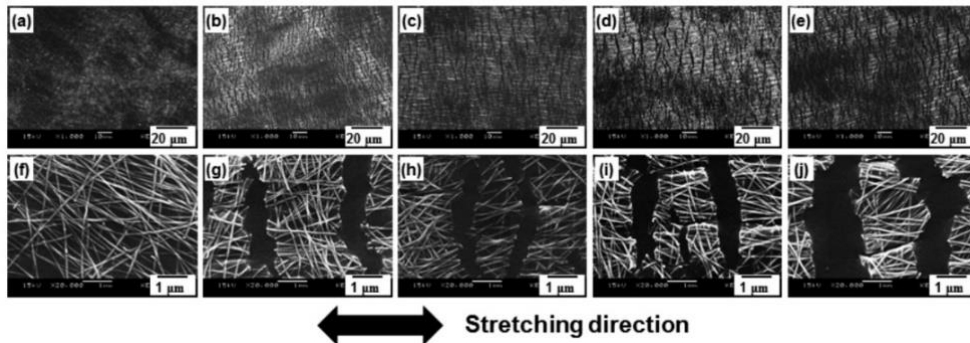


**Figure 9.** SEM micrographs for AgNWs deposited on hydroxylated PDMS: panels a–e are low magnification and panels f–j high magnification images. Panels a and f represent the pristine state, b and g the 25% strain stretched state, c and h the 50% strain stretched state, d and i the 75% strain stretched state, and e and j show images during stretching at 100% strain<sup>61</sup>.

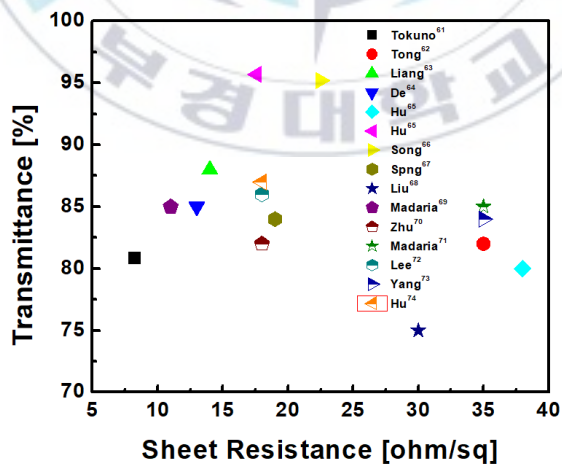


**Figure 10.** Sheet resistance and transmittance of silvernanowires based on references<sup>62–75</sup>.

### 2.3.5.1. AgNWs electrode challenge

#### a. High Surface Roughness

In spite of the outstanding performance of AgNWs, there are certain issues that need to be covered before AgNWs electrode applied as electrode. One of these most important issues is their surface roughness. After the deposition process, some nanowires stick out of the surface and some of them lie on top of each other, typically junctions on an electrode where 3 or more nanowires are stacked on top of one another, maximum peak-to-valley values can reach 3 times the diameter of the nanowires or more which increases surface roughness to a couple hundred nanometers<sup>76</sup>. For example in organic solar cells and OLED devices, the organic layer it should be thin (usually between 50-100 nm) and the rough surface of electrodes cause shorting of the devices<sup>12,77</sup>. Some methods have been introduced to reduce surface roughness of AgNWs, like laminating AgNWs films onto a soft material and making a polymer-nanowire composite, depositing a non-conductive polymer layer over the nanowire film followed by peel-off to expose the nanowire surfaces, and pressing nanowires on their substrate<sup>78</sup>.

b. Weak adhesion of AgNWs to the substrate

AgNWs has a problem with the weak adhesion to the substrate where without some treatments, the scratches and shear can occur on AgNWs on the surface easily. Some methods have been investigated in previous research. For example, oxygen plasma or ozone treatment and adding an additional layer on top of substrate can increase the AgNW's adhesion drastically<sup>18</sup>.

c. Instability of AgNWs

Other concern of AgNWs challenge is about their instability in air at elevated temperatures and under current flow. In the air, AgNWs reacting with a small amounts of sulfur and creating silver sulfide on the surface<sup>79</sup>. In addition, AgNWs are not stable in structures and at elevated temperatures (above 200 °C) or perhaps even less and their instability is accelerated and the cylindrical shape of the nanowires change to spheres<sup>65</sup>.

## Chapter 3

### EXPERIMENTAL DETAILS

#### 3.1. Experimental Section

As stretchable substrates, PDMS solutions (Sylgard 184, Dow Corning) were spin-coated on to polyethylene terephthalate (PET) at 300 rpm for 15 s and were subsequently annealed at 120 °C for 40 min in air ambient. The prepared PDMS substrates were pretreated by oxygen plasma for 15 m. For the surface modification of PDMS, 11-AA solutions (Sigma Aldrich) with a concentration of 0.08-0.16 wt.% in deionized water were spin-coated onto plasma-treated PDMS samples, and subsequently annealed at 100 °C for 10 m. The aqueous 0.5 wt.% AgNW aqueous dispersion (Nanopixys) was spin-coated onto PDMS substrates and was baked on the hot plate at 100 °C for 10 m. For the fabrication of AgNW/PEDOT: PSS composites, PEDOT: PSS (Clevios FET, Heraeus) was spin-coated on the AgNW films at 8000 rpm for 30 s and annealed at 120 °C for 10 m. The dried samples on the PDMS were peeled-off from the PET supporting substrates and cut into the required sample size. For the fabrication of transparent heaters, aluminum tapes were attached on both edges of the

AgNW or AgNW/PEDOT: PSS composites electrodes, which were wired to the power supply.

The ACEL device made with coated the Polyvinylidene fluoride(PVDF) with 530,000 MW from Sigma Aldrich was employed as flexible dielectric with dissolve PVDF in N,N-Dimethylformamide with 10 %w/w concentration, deposition by spin coating with spin speed 300 rpm for 10 s in above of electrode. And then continued with deposited ZnS (Zinc Sulfide) from Shanghai KPT Co., Ltd was used as emitting layer with mixed PDMS : ZnS = 60%:40%, deposition by spin coating with 1000 rpm spin speed for 20 s, AgNWs deposition for top electrode by spin coating with 1500 rpm spin speed for 30 s 2 layers, and continued with PDMS.

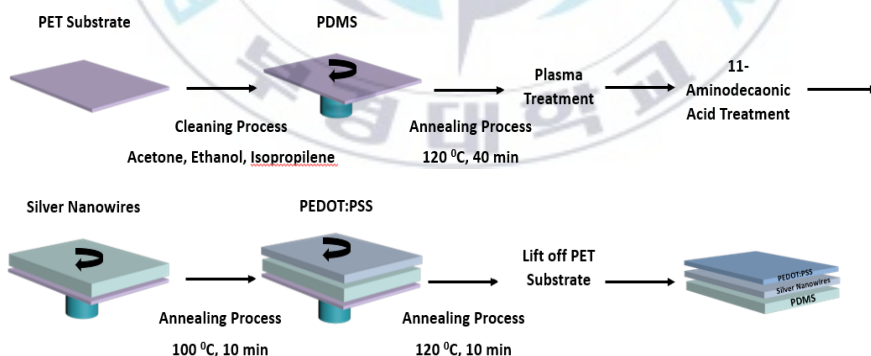


**Figure 11.** Schematic illustration of the fabrication process of electrode and Pre-treatment mechanism using Plasma Treatment and 11-Aminoundecanoic Acid

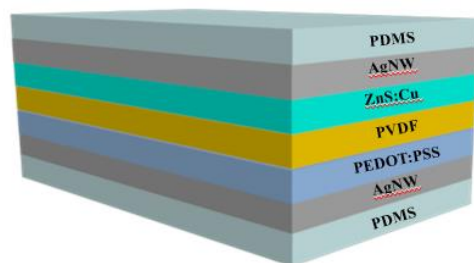


**Figure 12.** Schematic structure of ACEL devices.

### 3.2. Measurement

The sheet resistance was examined by van der Pauw method using a source-measure unit system (Keithley 2401). The transmittance was measured by UV–vis spectrophotometer (Optizen pop, MECASYS). The relative resistance under tensile strains was measured by a Keithley sourcemeter with a custom-made motion stage. For chemical stability tests, the TCEs were immersed in the solvent bath containing either ethanol or deionized water. DC voltages were applied in both sides of the electrodes by Keithley 2401 sourcemeter to obtain Joule heating. Thermal properties and images were obtained using an infrared (IR) camera (TiS45, Fluke). Performance of ACEL was measured by a goniometer equipped spectroradiometer (CS-2000, Minolta) and AC source-measure unit system.

## Chapter 4

### RESULT AND DISCUSSION

#### 4.1. Surface Modifier for Transparent Electrode

The AgNWs are deposited on PDMS which has a high transmittance, high elasticity, and outstanding biocompatibility. Figure 13 shows the schematic mechanism of the enhanced bonding properties using 11-AA with functional groups. Due to the weak van der Waals forces between AgNWs and the underlying PDMS substrate, a surface treatment step is required in order to produce strong, conformal bonds between the AgNW networks and the surfaces of PDMS. The plasma treatment for PDMS creates silanol groups (-OH) at the surface.<sup>13,18</sup> Additionally, we introduce 11-AA on plasma-treated PDMS substrates. The 11-AA has a functional group of primary amine (-NH<sub>2</sub>) which forms a hydrogen bond to AgNWs. Furthermore, the carboxyl group (COOH) of 11-AA forms a strong Si – O – Si covalent bond with PDMS substrates. As the interaction of covalent bond is known to be several orders of magnitude higher than van der Waals forces,<sup>13</sup> the resulting covalent and hydrogen bonds formed by 11-AA can

significantly improve the adhesion between nanowires and elastomeric substrate.

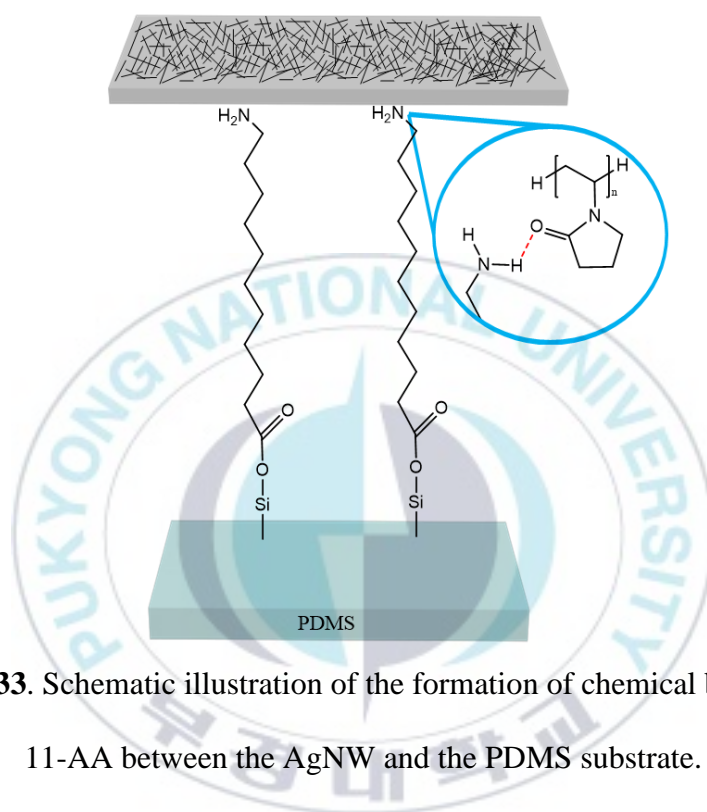


**Figure 133.** Schematic illustration of the formation of chemical bonds with 11-AA between the AgNW and the PDMS substrate.

#### 4.2. Optical and Electrical Properties of Transparent Electrode

AgNW was deposited using spin coating method with various spin speed, 1500 rpm, 3000 rpm and 5000 rpm at 30 s. The results of sheet resistance and transmittance were summarized in Figure 14. Based on the result in the graph, AgNW with 3000 rpm spin speed has the good performance than other, it was showed with sheet resistance 21.6  $\Omega$ /sq and

transmittance is 87.15 %. AgNW 3000 rpm spin speed has been chosen for the next investigation.

Figure 15a shows the behavior of the sheet and the transmittance of AgNW networks as a function of the concentration of 11-AA in deionized water. The sheet resistance of reference sample without 11-AA reveals a sheet resistance of 31.5  $\Omega/\text{sq}$  with a transmittance of 87.2 %. As the concentration of 11-AA increases, the sheet resistance decreases while the transmittance increases. The best performing AgNW network shows a sheet resistance of 26.0  $\Omega/\text{sq}$  and transmittance of 89.6 % at an 11-AA concentration of 0.14 wt.%. Such well-bonded AgNW network by 11-AA shows simultaneously enhanced electrical and optical properties. At a higher 11-AA concentration of 0.16 wt.%, the transmittance drops to 87.7 % while sheet resistance further decreases up to 24.6  $\Omega/\text{sq}$ . We also investigate the electrical and optical properties of combined AgNW-conductive PEDOT: PSS composites (c-AgNW) as shown in Figure 15b. Due to the overcoated conducting PEDOT: PSS films, the transmittances of c-AgNWs decrease compared to those of AgNW networks, with decreasing sheet resistances. The best performing c-AgNW film shows a sheet resistance of 19.9  $\Omega/\text{sq}$  with transmittance of 81.7 % at an 11-AA concentration of 0.14 wt.%. These

values of both AgNWs and c-AgNWs promise the excellent performances for the applications in optoelectronic devices.

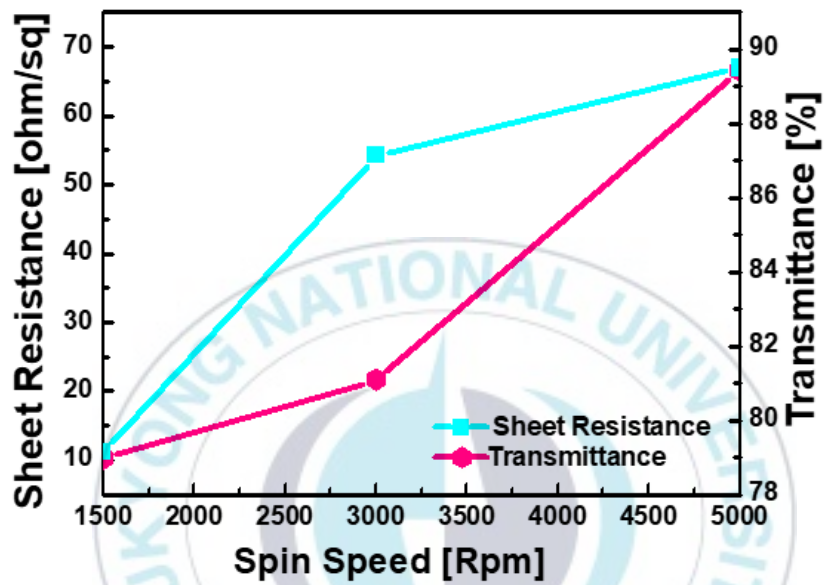
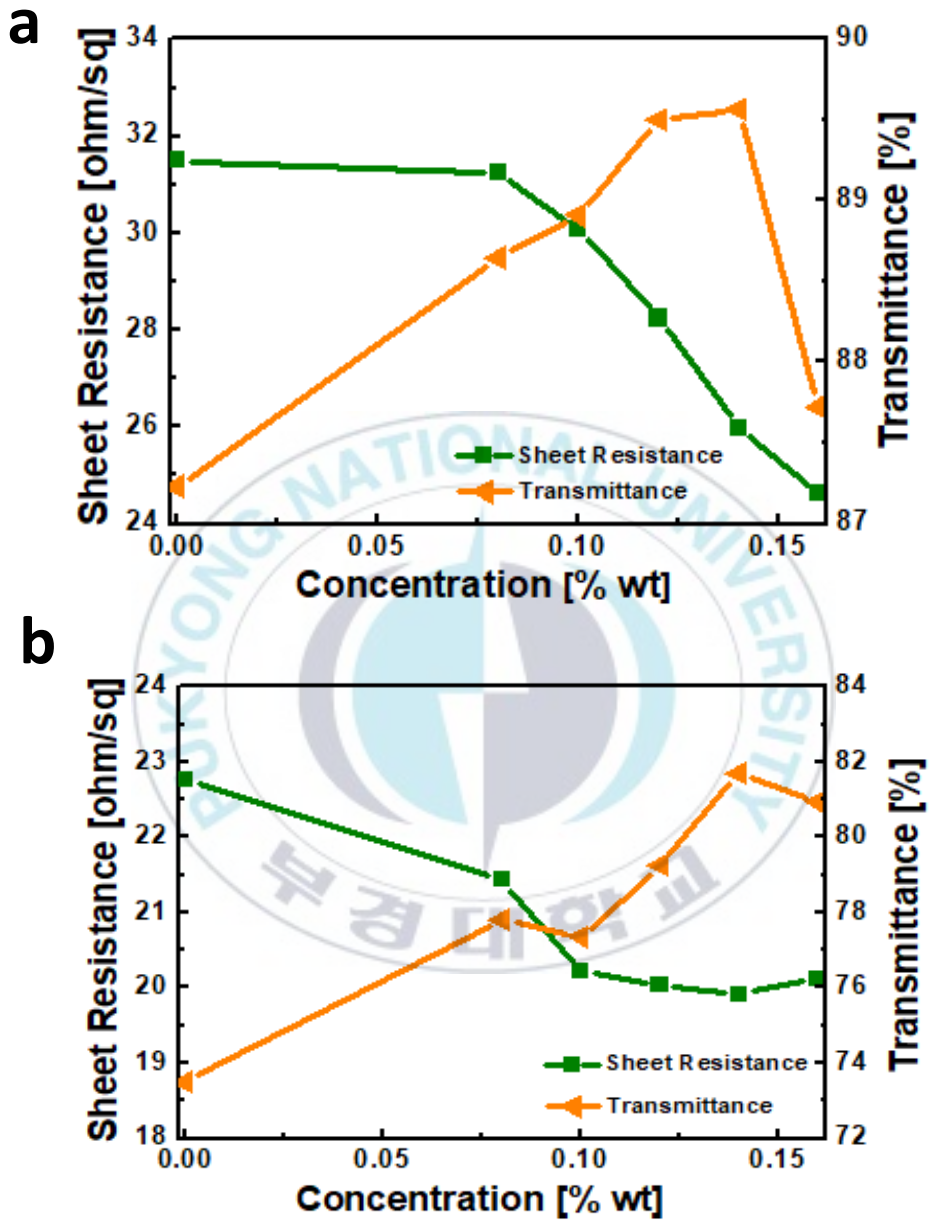


Figure 144. Sheet resistance and transmittance of AgNWs in various spin speed

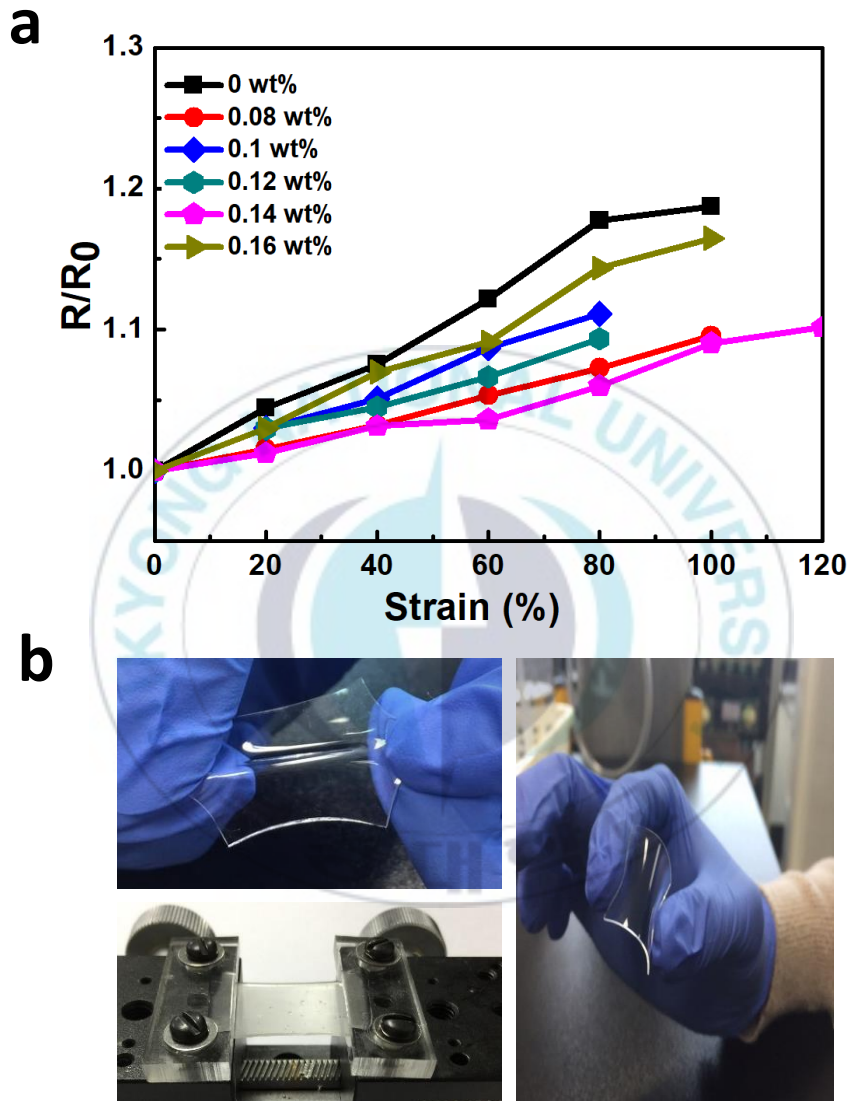


**Figure 15** Sheet resistance and transmittance of (a) AgNW and (b) c-AgNW treated with various concentration of 11-AA.

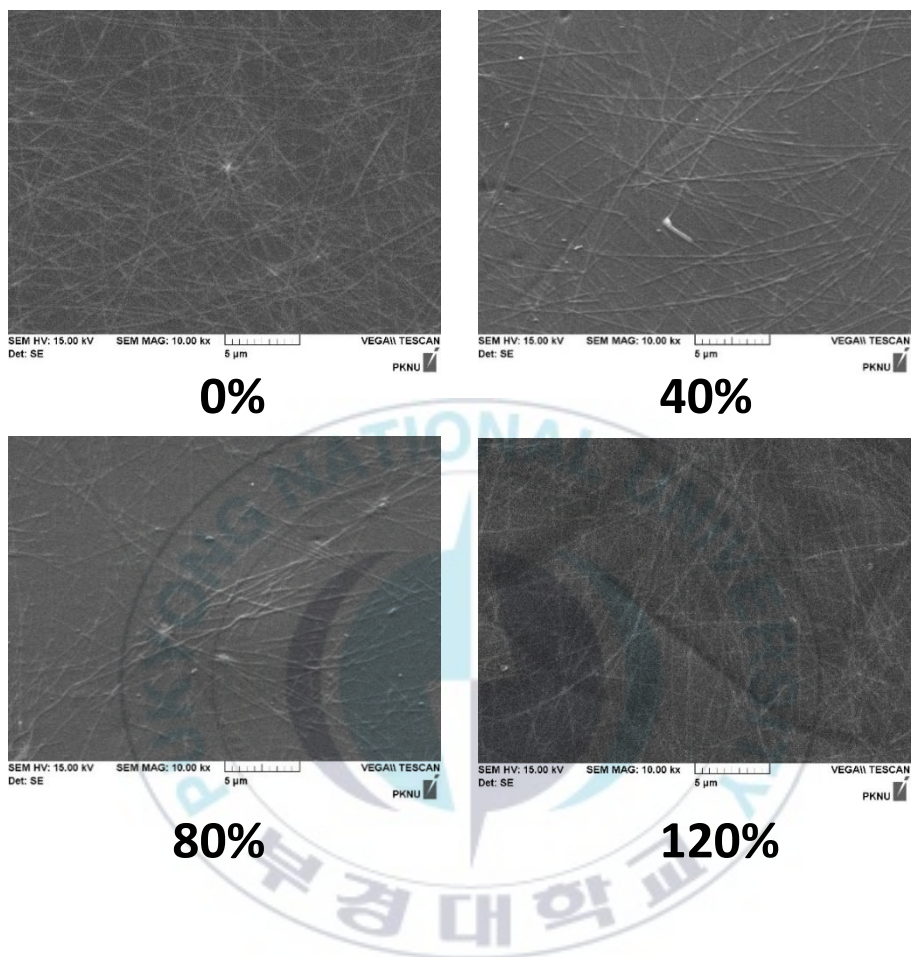
### 4.3. Mechanical Stability of the Electrode

Figure 16a shows the relative changes of the resistance ( $R/R_0$ , where  $R$  is the resistance under stretched condition,  $R_0$  is the initial resistance without strain) for c-AgNWs with respect to the concentration of 11-AA under the induced tensile strain. The resistance of films increases along with the applied strain. The c-AgNWs with an 11-AA concentration of 0.14 wt.% are stretched up to 120 %, resulting in the  $R/R_0$  increase by only 1.1-fold. The 11-AA introduced-c-AgNW networks reveal a remarkably suppressed resistance increase when the concentration of 11-AA increases. This suggests that 11-AA improves bonding between AgNWs and PDMS substrates and substantially suppresses the disconnection of wires under strains so that conducting pathways are retained. This superb stretchability using 11-AA is favorable for achieving high-performance stretchable electronics with minimal electrical loss. Figure 16b presents photographs of c-AgNW under stretching and bending conditions. The resistance increase of stretchable electrodes is caused by microscopic cracks together with the disconnection of nanowires. The crack of c-AgNW films treated with 11-AA (0.14 wt.%) is observed at the strain of 120 %, which leads to breaking of nanowire junctions and deteriorates the conductivity of stretchable

electrodes. It was supported by SEM image in 17. The tensile electrodes are measured by SEM to know the surface conditions. On initial conditions before stretching, an interconnection between AgNW perfectly make, but in 20% stretching of the electrode, the fracture phenomenon seems, and this will increase if the stretch is added again up to 120%. It is indicated if the position change or sliding of the nanowire may occur. This results in a change in the sheet resistance previously described, but an insignificant increase in sheet resistance is indicated as a result from the chemical treatment provided by the 11-AA causing strong bonds between AgNW and PDMS, so despite damage occur the electrode still can show excellent performance.



**Figure 16.** (a) Changes of resistances for c-AgNW treated with various concentration of 11-AA under tensile strains. (b) Photographs of c-AgNW under stretching and bending conditions.



**Figure 17.** SEM images of stretched c-AgNW treated with 0.14 wt.% of AA under various tensile strains.

#### 4.4. Chemical and Air Exposure Stability of the Electrode

We investigate chemical stabilities of AgNWs and c-AgNWs, both are treated with 11-AA (0.14 wt.%), against various conditions. Figure 18 shows the change in resistance of the electrodes dipped in ethanol. The resistance of the AgNW electrode dipped in ethanol is increased by 3.0-fold during a dipping time of 30 min. After 30 min, the AgNW networks are peeled-off from the supporting substrate. In contrast, c-AgNWs show the significantly improved chemical stability attributed to the protection effect of overcoated PEDOT: PSS. It is observed that the sheet resistance of c-AgNWs is only increased by about 1.7-fold during a dipping time of 60 min. This suggests that the interconnection between nanowires can be effectively preserved by the PEDOT: PSS protection layer against the penetration of chemicals. This enhanced stability is also observed for the films dipped in deionized water and the films stayed in air ambient (Figure 19 and 20). The resistances of c-AgNWs are only increased by 1.7 and 1.4-fold, while those of AgNWs are increased by 2.3 and 1.7-fold in deionized water (60 min) and air conditions (30 days), respectively. The greatly enhanced stability of c-AgNWs promises as a highly stable electrode for applications in wearable electronics.

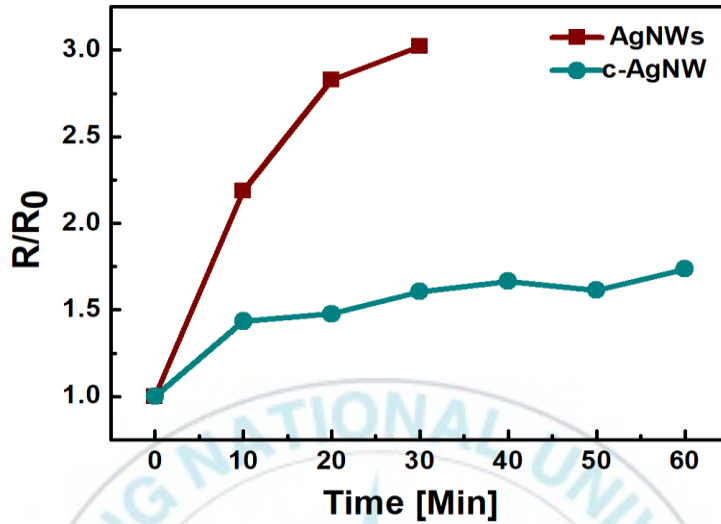


**Figure 18.** Changes of the normalized resistance for AgNW and c-AgNWs which is dipped in ethanol

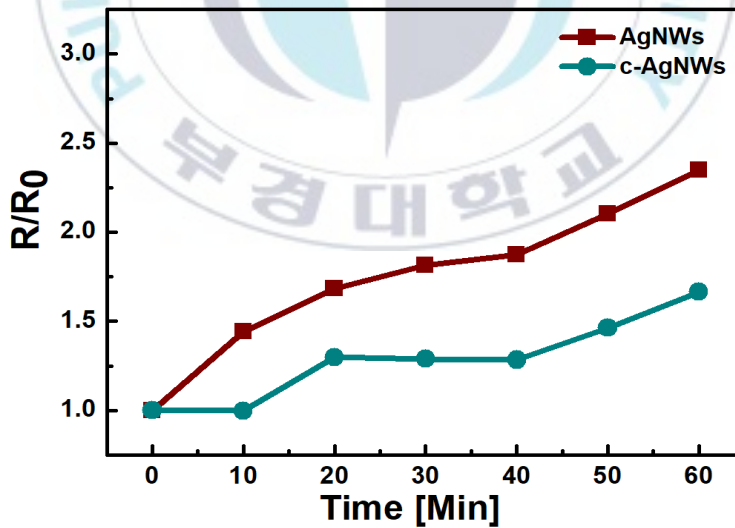


**Figure 19.** Changes of the normalized resistance for AgNW and c-AgNWs which is dipped in DIW

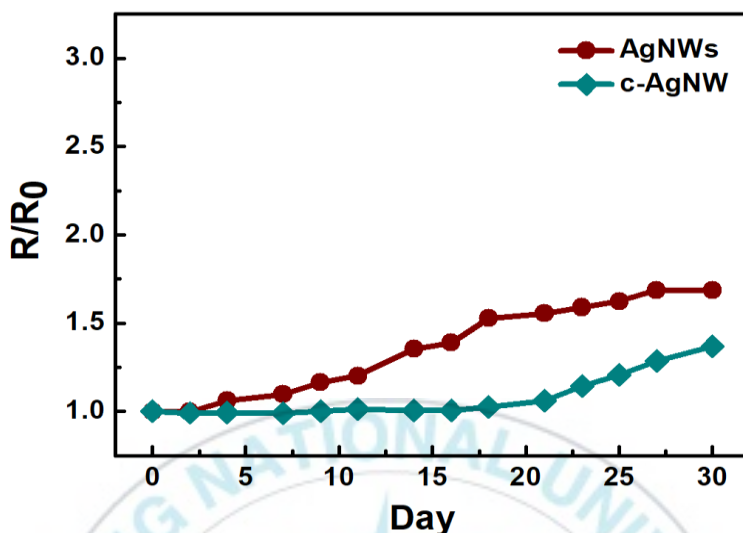


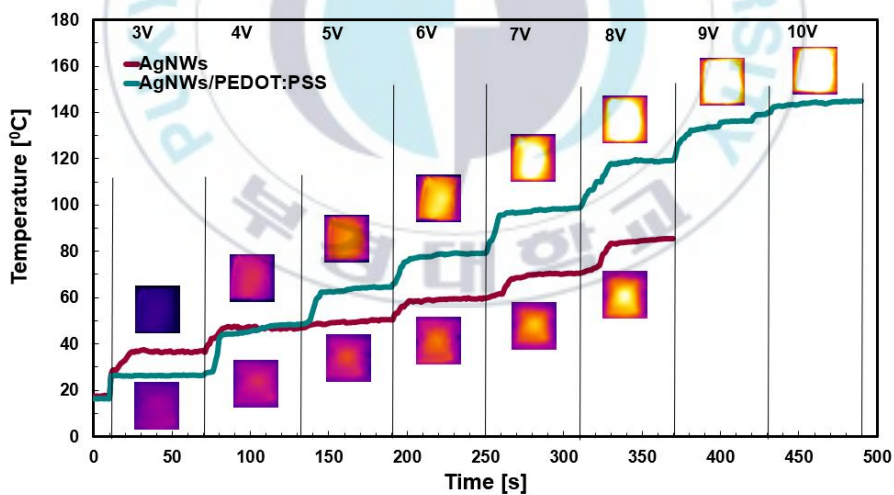
**Figure 19.** Changes of the normalized resistance for AgNW and c-AgNWs which is exposed in air ambient

#### 4.5. Performance of Transparent Electrode in Transparent Heater

The stretchable transparent heaters (STHs) are realized by AgNW and c-AgNWs with sheet resistances of 26 and 20  $\Omega$ /sq, respectively. All films for STHs are chemically treated with 11-AA (0.14 wt.%). Figure 21 presents the Joule

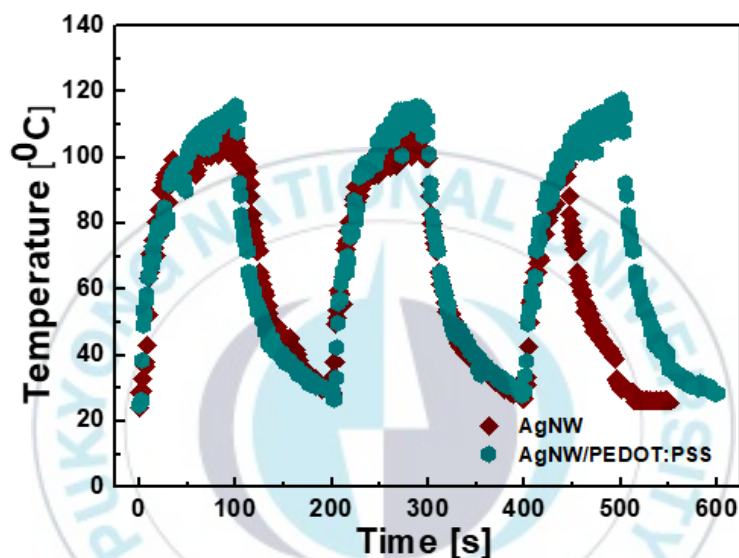
heating characteristics of the STHs, where a DC voltage is applied to the STHs and is increased by every 60 s from 3 to 10 V. The produced temperature clearly depends on the applied voltage. The STH with c-AgNWs generates the much higher temperature, reaching 140 °C, compared

to the AgNW-based STH at given voltages. Above 8 V, the failure of AgNW-based STH is observed, while STHs with c-AgNWs work until a high voltage of 10 V. These results indicate that the overcoated PEDOT: PSS layer in c-AgNW-based STHs enhances the formation of conducting pathways between nanowires and prevents from the failure of wire-to-wire contact at high temperatures. The operational stability of STHs under a constant bias voltage of 5 V is shown in Fig 22. STHs with c-AgNW exhibit more stable heating property in comparison with STHs with AgNW during the repetitive on-off cycles, indicating that the overcoated PEDOT: PSS



effectively suppresses the damage of the wires under repeated thermal stress.

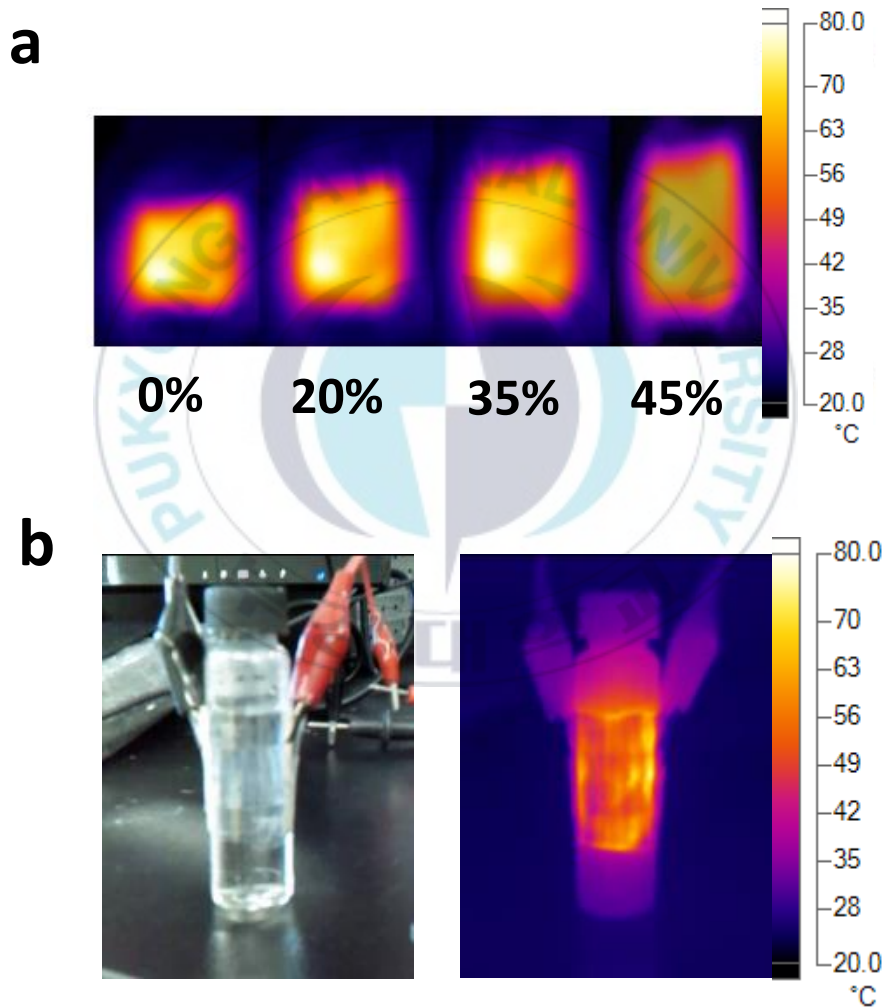
**Figure 20.** Temperature changes of STHs based on AgNW and c-AgNW as a function of time with increased applied voltages. Inset shows dynamic temperature control of the STHs with AgNW and c-AgNWs



**Figure 21.** The stability of heater with heating and cooling test with time interval 100 s in 10 min.

Figure 23a shows the IR images of the STHs based on c-AgNW treated with 0.14 wt.% 11-AA under various tensile strains at a constant voltage. The STHs with c-AgNWs stretched up to 45 % exhibit the outstanding stretchability and the uniform temperature distribution on the films. Figure 23b, 23c, 23d and 23e shows the superb elasticity of STHs

under various twisting and bending conditions. The STHs are easily twisted and attached on a bent surface, showing good conformal performance with various form factor.



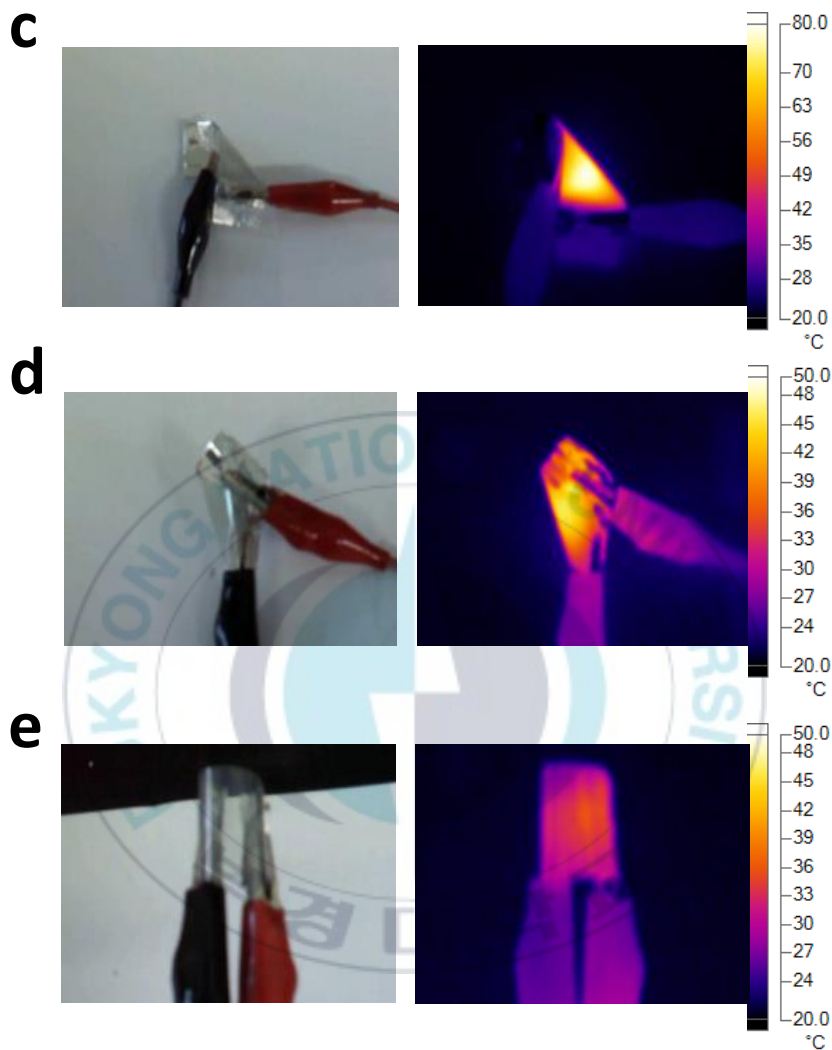


**Figure 22.** (a) IR image of the STH with c-AgNW under various tensile strains. (b) Photograph and IR image of STH with c-AgNW attached on a vial. (c) (d) (e) Photographs and IR images of STHs based on c-AgNW under twisting and bending conditions.

#### 4.6. Performance of Transparent Electrode in ACEL Device

In addition, we integrate c-AgNWs as a stretchable transparent electrode to the stretchable alternating current electroluminescence device in Figure 24, presenting a promising performance for applications in displays and lightings. Schematic layers of ACEL was shown in Figure 12 and fabrication of ACEL was explained in experimental details. ZnS was employed as an ACEL phosphor because of more stable and high luminance. ACEL devices were tested to get luminance with the various voltage at 400 Hz constant frequency, increasing voltage make luminance increase. The maximum luminance was exhibited at 500V with value was  $70.39 \text{ cd m}^{-2}$  and the light was emitted cyan color at 500 nm as showed in Figure 25a and 25b.

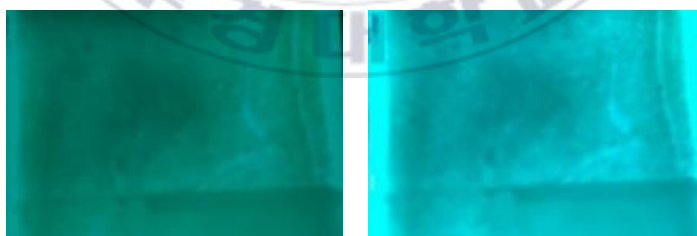


**Figure 23.** Photographs of ACEL device with a frequency 400 Hz (left) and 1000 Hz (right) and a voltage of 400 V.

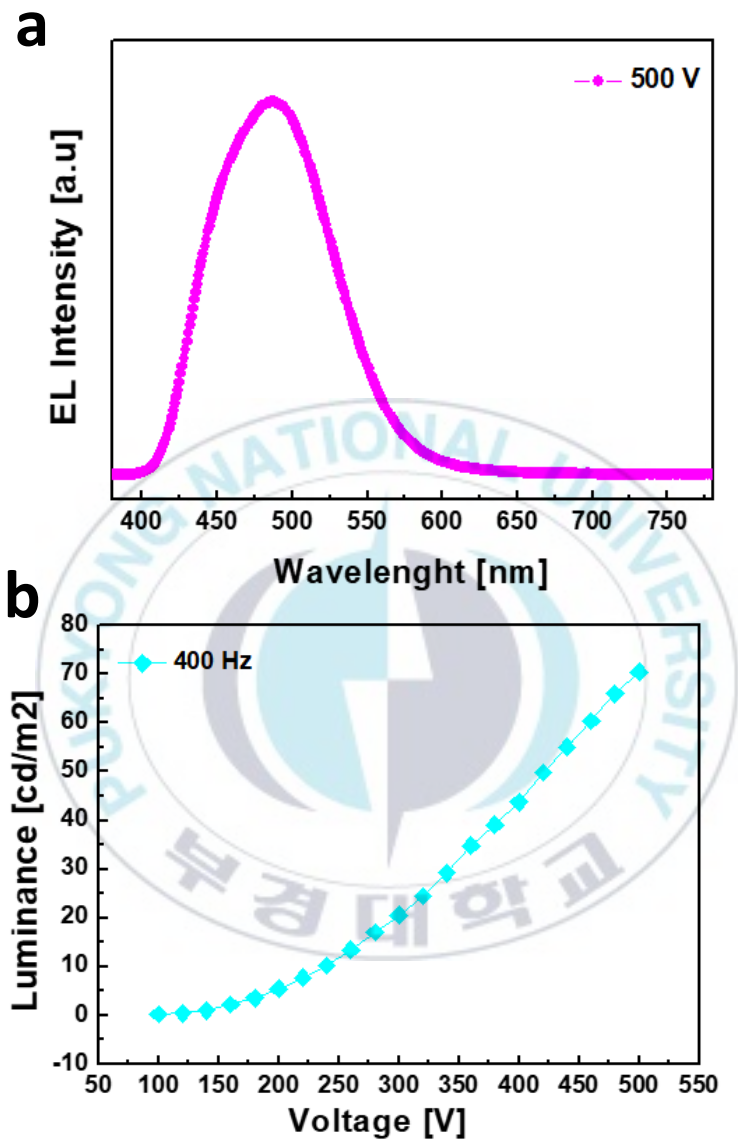


**Figure 24.** (a) Electroluminescent intensity (at 500 V) and (b) luminance (at 400 Hz) of the stretchable alternating current electroluminescence device.

## Chapter 5

### CONCLUSION

In conclusion, the electrical and optical properties of AgNW films are simultaneously enhanced by the introduction 11-AA, forming a strong chemical bond between nanowires and PDMS. In addition, the embedment of AgNW into the conductive PEDOT: PSS film provides the remarkably improved chemical stability and mechanical stability as the overcoated PEDOT: PSS effectively protects chemical penetration and suppresses mechanical stress in the wire junctions. The STHs prepared with c-AgNWs exhibit much enhanced and stabilized Joule heating performances. We believe that the surface modification strategy investigated here has high availability and can be a key step towards future wearable applications.

## Chapter 6

### REFERENCES

1. McCoul, D., Hu, W., Gao, M., Mehta, V. & Pei, Q. Recent Advances in Stretchable and Transparent Electronic Materials. *Adv. Electron. Mater.* **2**, 1–51 (2016).
2. Emmott, C. J. M., Urbina, A. & Nelson, J. Environmental and economic assessment of ITO-free electrodes for organic solar cells. *Sol. Energy Mater. Sol. Cells* **97**, 14–21 (2012).
3. Ellmer, K. Past achievements and future challenges in the development of optically transparent electrodes. *Nat. Photonics* **6**, 809–817 (2012).
4. Huang, X., Zeng, Z., Fan, Z., Liu, J. & Zhang, H. Graphene-based electrodes. *Adv. Mater.* **24**, 5979–6004 (2012).
5. Han, T.-H. *et al.* Extremely efficient flexible organic light-emitting diodes with modified graphene anode. *Nat. Photonics* **6**, 105–110 (2012).
6. Rowell, M. W. *et al.* Organic solar cells with carbon nanotube network electrodes. *Appl. Phys. Lett.* **88**, (2006).
7. Hu, L., Li, J., Liu, J., Gruner, G. & Marks, T. Flexible organic light-emitting diodes with transparent carbon nanotube electrodes: Problems and solutions. *Nanotechnology* **21**, (2010).
8. Kim, Y. H. *et al.* Highly conductive PEDOT:PSS electrode with optimized solvent and thermal post-treatment for ITO-free organic solar cells. *Adv. Funct. Mater.* **21**, 1076–1081 (2011).
9. Kim, Y. H. *et al.* Achieving high efficiency and improved stability in ITO-free transparent organic light-emitting diodes with conductive polymer electrodes. *Adv. Funct. Mater.* **23**, 3763–3769 (2013).
10. Kim, Y. H., Müller-Meskamp, L. & Leo, K. Ultratransparent polymer/semitransparent silver grid hybrid electrodes for small-molecule organic solar cells. *Adv. Energy Mater.* **5**, 1–5 (2015).
11. Kim, Y. H., Schubert, S., Timmreck, R., Müller-Meskamp, L. & Leo,

- K. Collecting the Electrons on n-Doped Fullerene C 60 Transparent Conductors for All-Vacuum-Deposited Small-Molecule Organic Solar Cells. *Adv. Energy Mater.* **3**, 1551–1556 (2013).
12. Kim, D. W., Han, J. W., Lim, K. T. & Kim, Y. H. Highly Enhanced Light-Outcoupling Efficiency in ITO-Free Organic Light-Emitting Diodes Using Surface Nanostructure Embedded High-Refractive Index Polymers. *ACS Appl. Mater. Interfaces* **10**, 985–991 (2018).
  13. Guo, C. F., Chen, Y., Tang, L., Wang, F. & Ren, Z. Enhancing the Scratch Resistance by Introducing Chemical Bonding in Highly Stretchable and Transparent Electrodes. *Nano Lett.* **16**, 594–600 (2016).
  14. Ye, S., Rathmell, A. R., Chen, Z., Stewart, I. E. & Wiley, B. J. Metal nanowire networks: The next generation of transparent conductors. *Adv. Mater.* **26**, 6670–6687 (2014).
  15. Cheng, T., Zhang, Y., Lai, W. Y. & Huang, W. Stretchable thin-film electrodes for flexible electronics with high deformability and stretchability. *Adv. Mater.* **27**, 3349–3376 (2015).
  16. Sannicolo, T. *et al.* Metallic Nanowire-Based Transparent Electrodes for Next Generation Flexible Devices: a Review. *Small* **12**, 6052–6075 (2016).
  17. Trung, T. Q. & Lee, N. E. Recent Progress on Stretchable Electronic Devices with Intrinsically Stretchable Components. *Adv. Mater.* **29**, (2017).
  18. Lee, H., Lee, K., Park, J. T., Kim, W. C. & Lee, H. Well-ordered and high density coordination-type bonding to strengthen contact of silver nanowires on highly stretchable polydimethylsiloxane. *Adv. Funct. Mater.* **24**, 3276–3283 (2014).
  19. Lipomi, D. J. & Bao, Z. Stretchable, elastic materials and devices for solar energy conversion. *Energy Environ. Sci.* **4**, 3314 (2011).
  20. Szablewski, L., Ghanbarzadeh, B. & Almasi, H. World ' s largest Science , Technology & Medicine Open Access book publisher c. *RFID Technol. Secur. Vulnerabilities, Countermeas.* 75–100 (2016). doi:10.5772/711

21. Zweibel, K. *The Terawatt Challenge for Thin Film Photovoltaics. Thin Film Solar Cells Fabrication, Characterization and Applications* (2006). doi:10.1002/0470091282.ch11
22. Lee, H., Kim, M., Kim, I. & Lee, H. Flexible and Stretchable Optoelectronic Devices using Silver Nanowires and Graphene. *Adv. Mater.* **28**, 4541–4548 (2016).
23. Lee, T. *et al.* Transparent ITO mechanical crack-based pressure and strain sensor. *J. Mater. Chem. C* **4**, 9947–9953 (2016).
24. Hecht, D. S., Hu, L. & Irvin, G. Emerging transparent electrodes based on thin films of carbon nanotubes, graphene, and metallic nanostructures. *Adv. Mater.* **23**, 1482–1513 (2011).
25. Cheong, H. G., Song, D. W. & Park, J. W. Transparent film heaters with highly enhanced thermal efficiency using silver nanowires and metal/metal-oxide blankets. *Microelectron. Eng.* **146**, 11–18 (2015).
26. Thirumoorthi, M. & Thomas Joseph Prakash, J. Structure, optical and electrical properties of indium tin oxide ultra thin films prepared by jet nebulizer spray pyrolysis technique. *J. Asian Ceram. Soc.* **4**, 124–132 (2016).
27. Park, J. H. *et al.* The effect of post-annealing on Indium Tin Oxide thin films by magnetron sputtering method. *Appl. Surf. Sci.* **307**, 388–392 (2014).
28. Terzini, E., Thilakan, P. & Minarini, C. Properties of ITO thin films deposited by RF magnetron sputtering at elevated substrate temperature. *Mater. Sci. Eng. B* **77**, 110 (2000).
29. Daoudi, K. *et al.* Tin-doped indium oxide thin films deposited by sol-gel dip-coating technique. *Mater. Sci. Eng. C* **21**, 313–317 (2002).
30. Kesim, M. T. & Durucan, C. Indium tin oxide thin films elaborated by sol-gel routes: The effect of oxalic acid addition on optoelectronic properties. *Thin Solid Films* **545**, 56–63 (2013).
31. Nunes de Carvalho, C. *et al.* Effect of rf power on the properties of ITO thin films deposited by plasma enhanced reactive thermal evaporation on unheated polymer substrates. *J. Non. Cryst. Solids* **299–302**, 1208–1212 (2002).

32. Hanus, F., Jadin, A. & Laude, L. D. Pulsed laser deposition of high quality ITO thin films. *Appl. Surf. Sci.* **96–98**, 807–810 (1996).
33. Petukhov, I. A. *et al.* Pulsed laser deposition of conductive indium tin oxide thin films. *Inorg. Mater.* **48**, 1020–1025 (2012).
34. Hwang, M. S., Jeong, B. Y., Moon, J., Chun, S. K. & Kim, J. Inkjet-printing of indium tin oxide (ITO) films for transparent conducting electrodes. *Mater. Sci. Eng. B Solid-State Mater. Adv. Technol.* **176**, 1128–1131 (2011).
35. de la L. Olvera, M., Maldonado, A., Asomoza, R., Konagai, M. & Asomoza, M. Growth of textured ZnO:In thin films by chemical spray deposition. *Thin Solid Films* **229**, 196–200 (1993).
36. Letierrier, Y. *et al.* Mechanical integrity of transparent conductive oxide films for flexible polymer-based displays. *Thin Solid Films* **460**, 156–166 (2004).
37. Cui, J. *et al.* Indium tin oxide alternatives - High work function transparent conducting oxides as anodes for organic light-emitting diodes. *Adv. Mater.* **13**, 1476–1480 (2001).
38. Phillips, J. M. *et al.* Transparent conducting thin films of GaInO<sub>3</sub>. *Appl. Phys. Lett.* **65**, 115–117 (1994).
39. Minami, T. Transparent conducting oxide semiconductors for transparent electrodes. *Semicond. Sci. Technol.* **20**, (2005).
40. Carter, G., Nobes, M. & Armour, D. The erosion energy efficiency of sputtering. *Vacuum* **32**, 509–512 (1982).
41. Rafique, I., Kausar, A., Anwar, Z. & Muhammad, B. Exploration of Epoxy Resins, Hardening Systems, and Epoxy/Carbon Nanotube Composite Designed for High Performance Materials: A Review. *Polym. - Plast. Technol. Eng.* **55**, 312–333 (2016).
42. Prasek, J. *et al.* Methods for carbon nanotubes synthesis—review. *J. Mater. Chem.* **21**, 15872 (2011).
43. Huang, Z.-D. *et al.* Self-assembled reduced graphene oxide/carbon nanotube thin films as electrodes for supercapacitors. *J. Mater. Chem.* **22**, 3591 (2012).
44. Kim, Y., Lee, H. R., Saito, T. & Nishi, Y. Ultra-thin and high-

- response transparent and flexible heater based on carbon nanotube film. *Appl. Phys. Lett.* **110**, (2017).
45. Dan B.a Irvin, G. C. . P. M. . Continuous and scalable fabrication of transparent conducting carbon nanotube films. *ACS Nano* **3**, 835–843 (2009).
  46. Wang, S. J., Geng, Y., Zheng, Q. & Kim, J. K. Fabrication of highly conducting and transparent graphene films. *Carbon N. Y.* **48**, 1815–1823 (2010).
  47. Stankovich, S. *et al.* Stable aqueous dispersions of graphitic nanoplatelets via the reduction of exfoliated graphite oxide in the presence of poly(sodium 4-styrenesulfonate). *J. Mater. Chem.* **16**, 155–158 (2006).
  48. Ions, D. *et al.* Graphene Oxide Papers Modified by. *ACS Nano* **2**, 572–8 (2008).
  49. Watcharotone, S. *et al.* Graphene- Silica Composite Thin Films as Transparent Conductors. *Nano Lett.* **7**, 1888–1892 (2007).
  50. Yi, M. & Shen, Z. A review on mechanical exfoliation for the scalable production of graphene. *J. Mater. Chem. A* **3**, 11700–11715 (2015).
  51. Seo, Y. K. *et al.* Efficient ITO-free organic light-emitting diodes comprising PEDOT:PSS transparent electrodes optimized with 2-ethoxyethanol and post treatment. *Org. Electron. physics, Mater. Appl.* **42**, 348–354 (2017).
  52. Seo, Y. K. *et al.* Enhanced electrical properties of PEDOT:PSS films using solvent treatment and its application to ITO-free organic light-emitting diodes. *J. Lumin.* **187**, 221–226 (2017).
  53. Wang, Q., Ahmadian-Yazdi, M. R. & Eslamian, M. Investigation of morphology and physical properties of modified PEDOT: PSS films made via in-situ grafting method. *Synth. Met.* **209**, 521–527 (2015).
  54. Xia, Y. & Ouyang, J. PEDOT:PSS films with significantly enhanced conductivities induced by preferential solvation with cosolvents and their application in polymer photovoltaic cells. *J. Mater. Chem.* **21**, 4927 (2011).
  55. Fan, B., Mei, X. & Ouyang, J. Significant Conductivity Enhancement

- of Conductive Poly(3,4-ethylenedioxythiophene):Poly(styrenesulfonate) Films by Adding Anionic Surfactants into Polymer Solution. *Macromolecules* **41**, 5971–5973 (2008).
56. Wang, Q. & Eslamian, M. Improving uniformity and nanostructure of solution-processed thin films using ultrasonic substrate vibration post treatment (SVPT). *Ultrasonics* **67**, 55–64 (2016).
  57. Xia, Y. & Ouyang, J. Highly conductive PEDOT:PSS films prepared through a treatment with geminal diols or amphiphilic fluoro compounds. *Org. Electron. physics, Mater. Appl.* **13**, 1785–1792 (2012).
  58. Xia, Y., Sun, K. & Ouyang, J. Solution-processed metallic conducting polymer films as transparent electrode of optoelectronic devices. *Adv. Mater.* **24**, 2436–2440 (2012).
  59. Gueye, M. N., Carella, A., Demadrille, R. & Simonato, J. P. All-Polymeric Flexible Transparent Heaters. *ACS Appl. Mater. Interfaces* **9**, 27250–27256 (2017).
  60. Coskun, S., Aksoy, B. & Unalan, H. E. Polyol synthesis of silver nanowires: An extensive parametric study. *Cryst. Growth Des.* **11**, 4963–4969 (2011).
  61. You, B., Kim, Y., Ju, B. K. & Kim, J. W. Highly Stretchable and Waterproof Electroluminescence Device Based on Superstable Stretchable Transparent Electrode. *ACS Appl. Mater. Interfaces* **9**, 5486–5494 (2017).
  62. Tokuno, T. *et al.* Fabrication of silver nanowire transparent electrodes at room temperature. *Nano Res.* **4**, 1215–1222 (2011).
  63. Tong, K., Chen, D., Liang, J. & Pei, Q. Stretchable Transparent Electrodes Based on Silver Nanowires. 139–142 (2017).
  64. Madaria, A. R., Kumar, A. & Zhou, C. Large scale, highly conductive and patterned transparent films of silver nanowires on arbitrary substrates and their application in touch screens. *Nanotechnology* **22**, (2011).
  65. Lee, J. Y., Connor, S. T., Cui, Y. & Peumans, P. Solution-processed

- metal nanowire mesh transparent electrodes. *Nano Lett.* **8**, 689–692 (2008).
66. Yang, L. *et al.* Solution-Processed Flexible Polymer Solar Cells with Silver Nanowire Electrodes. *ACS Appl. Mater. Interfaces* **3**, 4075–4084 (2011).
  67. Hu, W. *et al.* Intrinsically stretchable transparent electrodes based on silver-nanowire-crosslinked-polyacrylate composites. *Nanotechnology* **23**, (2012).
  68. Liang, J. *et al.* Silver nanowire percolation network soldered with graphene oxide at room temperature and its application for fully stretchable polymer light-emitting diodes. *ACS Nano* **8**, 1590–1600 (2014).
  69. De, S. *et al.* Silver Nanowire Networks as Flexible ., **3**, 1767–1774 (2009).
  70. Hu, L., Kim, H. S., Lee, J., Peumans, P. & Cui, Y. Scalable Coating and Properties of transparent Ag nanowire. *ACS Nano* **4**, 2955–2963 (2010).
  71. Song, M. *et al.* Highly efficient and bendable organic solar cells with solution-processed silver nanowire electrodes. *Adv. Funct. Mater.* **23**, 4177–4184 (2013).
  72. Song, T.-B. *et al.* Highly Robust Silver Nanowire Network for Transparent Highly Robust Silver Nanowire Network for Transparent Electrode. *ACS Appl. Mater. Interfaces* **7**, 24601–24607 (2015).
  73. Liu, S., Ho, S. & So, F. Novel Patterning Method for Silver Nanowire Electrodes for Thermal-Evaporated Organic Light Emitting Diodes. *ACS Appl. Mater. Interfaces* **8**, 9268–9274 (2016).
  74. Madaria, A. R., Kumar, A., Ishikawa, F. N. & Zhou, C. Uniform, highly conductive, and patterned transparent films of a percolating silver nanowire network on rigid and flexible substrates using a dry transfer technique. *Nano Res.* **3**, 564–573 (2010).
  75. Zhu, R. *et al.* Fused silver nanowires with metal oxide nanoparticles and organic polymers for highly transparent conductors. *ACS Nano* **5**, 9877–9882 (2011).

76. Choi, D. Y., Kang, H. W., Sung, H. J. & Kim, S. S. Annealing-free, flexible silver nanowire–polymer composite electrodes via a continuous two-step spray-coating method. *Nanoscale* **5**, 977–983 (2013).
77. Yu, Z., Li, L., Zhang, Q., Hu, W. & Pei, Q. Silver nanowire-polymer composite electrodes for efficient polymer solar cells. *Adv. Mater.* **23**, 4453–4457 (2011).
78. Hu, L., Kim, H. S., Lee, J. Y., Peumans, P. & Cui, Y. Scalable coating and properties of transparent, flexible, silver nanowire electrodes. *ACS Nano* **4**, 2955–2963 (2010).
79. Elechiguerra, J. L. *et al.* Corrosion at the nanoscale: The case of silver nanowires and nanoparticles. *Chem. Mater.* **17**, 6042–6052 (2005).

